Q. Jl R. astr. Soc. (1990), **31**, 305–331

Gravitational lenses*

R.D.Blandford
Theoretical Astrophysics, California Institute of Technology, Pasadena, CA 91125, U.S.A.

(Received 1990 February 27)

SUMMARY

The imaging of cosmologically distant point and extended sources, specifically quasars, galaxies and radio sources by intervening masses, is described. Particular attention is paid to formalisms which allow one to understand the qualitative principles governing image formation and procedures which furnish information on the structure of the source and the lens. The importance of caustics is emphasized, particularly their role in the formation of highly magnified images. Although gravitational lenses have been welcomed as powerful probes of dark matter, cosmographic tools, and giant telescopes, they have not yet fulfilled their promise in any of these areas. Despite this, it is argued that gravitational lenses will soon become important tools for extragalactic astronomy. It is suggested that large-scale structure can also be probed using gravitational distortion of the images of high redshift galaxies.

1 INTRODUCTION

1.1 *History*

Just over 70 years ago, on 1919 November 6, at a joint meeting of the Royal Astronomical and Royal Societies, Dyson, the Astronomer Royal, announced the results of an experiment to measure the deflection of starlight passing by the limb of the Sun during solar eclipse (Dyson 1919). The answer, which had been eagerly anticipated, was consistent with the prediction of the general theory of relativity, $4GM_\odot/R_\odot c^2 = 1{\cdot}75''$ and inconsistent with a naive application of Newton's theory which gave half this value (e.g. Wayman & Murray 1989). The consequences of this announcement were widespread acceptance of the theory among physicists and public notoriety for its author, Albert Einstein. For Eddington (who had helped organize the observation to avoid compromising his pacifism), the results were hardly a surprise. He, like Einstein, was already convinced of the theory's validity. In an earlier note (Eddington 1919), he had given a pedagogical discussion of the relativistic calculation by pointing out that, in the weak-field limit, curved spacetime behaved as if it were flat but endowed with a refractive index, $1-2\varphi/c^2$, where φ is the gravitational potential. As φ is negative, light waves are refracted toward the source of the potential just as they are refracted in the objective lens of a telescope. This was language astronomers could understand. Although Riemannian geometry is less intimidating 70 years later, Eddington's prescription will be a good place for us to start.

* George Darwin Lecture, delivered 1989 December 8.

As far as I know, the earliest suggestion that a gravitational lens could be strong enough to create more than one image was due to Lodge, who had earlier (Lodge 1919a) expressed the hope that Newtonian theory would be vindicated (along with his ethereal convictions). Despite the disappointment of the result he rushed off a paper to *Nature* (Lodge 1919b) defending a Newtonian explanation and pointing out that the Sun could act as a lens and bring light to a focus at a distance of seventeen times Neptune's orbit.

Over the next 60 years, the idea that a gravitational field could focus light was developed and observational evidence for the effect sought by several astronomers, including Chwolson (1924), Einstein (1936), Zwicky (1937), and in the modern era, Klimov (1963), Refsdal (1964), Liebes (1964), Barnothy (1965), Press & Gunn (1973) and Bourassa & Kantowski (1975). It was realized early on that stars were unlikely to form multiple images and that galaxies were far more promising. In addition, many of the geometrical optics properties of gravitational lenses were understood. As was also the case with the discovery of neutron stars, my theoretical colleagues had anticipated a creditable fraction of what was to come. (I claim no credit. As a graduate student, I shared an office with Nigel Sanitt, who wrote a thesis on this topic, and I can ruefully recall berating him for working on a phenomenon that was unlikely ever to be observed.)

In order to fix ideas, let us make some order of magnitude estimates. If we adopt Eddington's prescription, we find that the deflection angle α for a light ray from a background source is roughly φ/c^2. We can therefore invoke the virial theorem to express the angular displacement of a background quasar by an intervening galaxy in terms of its radial velocity dispersion, σ,

$$\alpha \sim \left(\frac{4\pi\sigma^2}{c^2}\right) \sim 2'' \left(\frac{\sigma}{300 \text{ km sec}^{-1}}\right)^2, \qquad (1)$$

where the coefficient 4π comes from a more careful estimate for an isothermal sphere. As a typical bright galaxy velocity dispersion is ~ 300 km sec^{-1}, it was found that it should be possible to split the images optically under conditions of good seeing. The associated impact parameter for a cosmologically distant lens will be roughly 10 kpc, well within the galaxy. For a distant, rich cluster of galaxies, with a velocity dispersion $\sigma \sim 1000$ km sec^{-1}, the image splitting will be $\sim 20''$ and the associated impact parameter will be ~ 200 kpc, comparable with a typical cluster core radius.

Gravitational lensing became an observational subject in 1979 when the Society's treasurer, Dennis Walsh, and his colleagues Carswell and Weymann announced the discovery of the so-called double quasar Q0957+561 (Fig. 1). (The tortuous path to this well-deserved discovery has recently been mapped by Walsh (1989) and this should be required reading for those who believe that scientific discovery happens in an orderly manner.) What Walsh, Carswell & Weymann (1979) found was two images separated by $6''$ of a $z = 1{\cdot}4$ quasar containing common emission and absorption lines. Their proposal, that light from the quasar had followed two separate paths to us, was vindicated with the discovery by Peter Young and others (Young *et al.* 1980) of a $z = 0{\cdot}36$ giant galaxy lying between the two images and a surrounding cluster. In subsequent modelling (Young *et al.* 1981), it was found that the combined gravitational deflection of the galaxy and the cluster

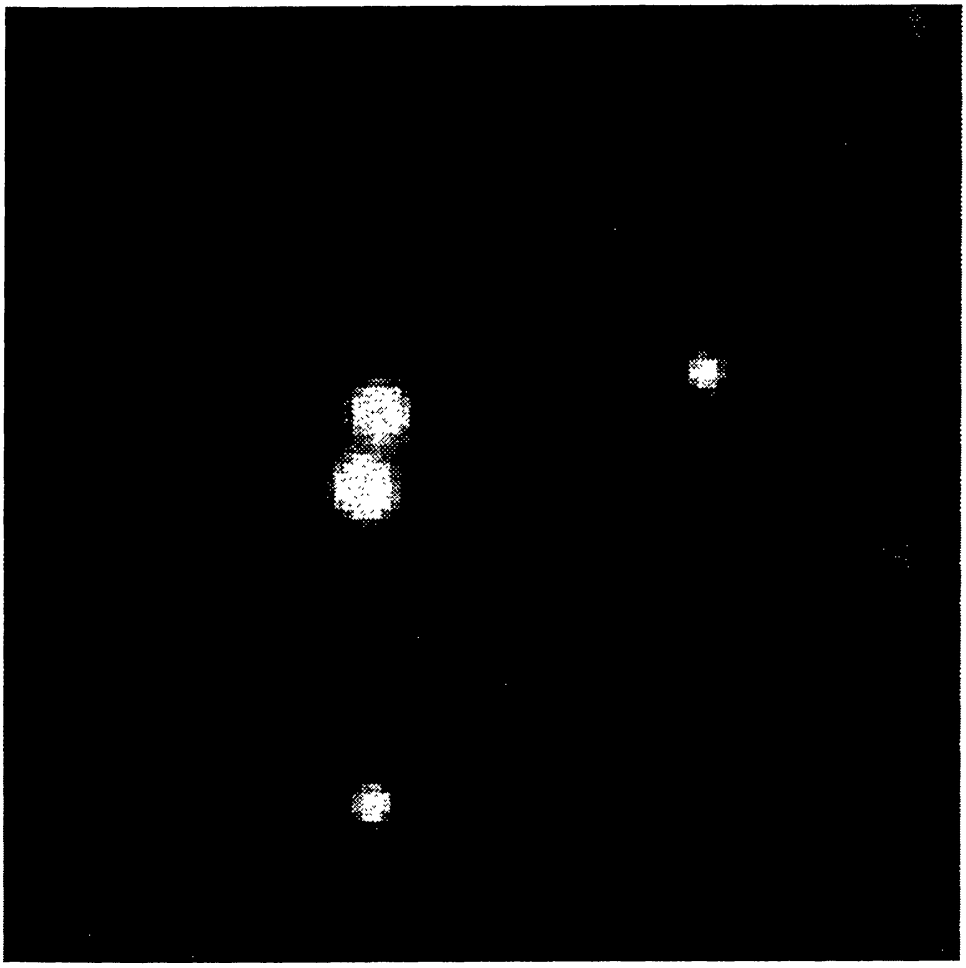

FIG. 1. Photograph of the first multiply-imaged quasar to be discovered, Q0957+561. The two bright images of a single background quasar in the centre are superposed on a fainter nebulosity which is an intervening galaxy. The extended fainter images are smaller galaxies belonging to the same cluster. All the galaxies contribute to the lens. (Image courtesy of E.Falco & R.Schild.)

could account for the image locations. Further evidence for gravitational lensing came with the discovery by Porcas *et al.* (1981) of similar VLBI radio structure at the sites of the two optical images.

The importance of rich clusters of galaxies for gravitational lensing was dramatically demonstrated with the discovery in 1986 of a long circular arc with angular radius $\sim 25''$ and angular length $\sim 20''$ in Abell 370 by Soucail *et al.* (1987) and Lynds & Petrosian (1986) (Fig. 2). This arc is now believed to be a highly distorted background galaxy, in this case with a measured redshift of $z = 0{\cdot}72$, about twice the cluster redshift $z = 0{\cdot}37$ (e.g. Paczyński 1987).

In 1987, a third type of lens, a ring, MG1131+0456, was discovered by Hewitt *et al.* (1988). In this instance, radio waves from a distant compact radio source are deflected by an intervening galaxy to form an almost complete elliptical ring of diameter about $2''$. Modelling of arcs and rings has

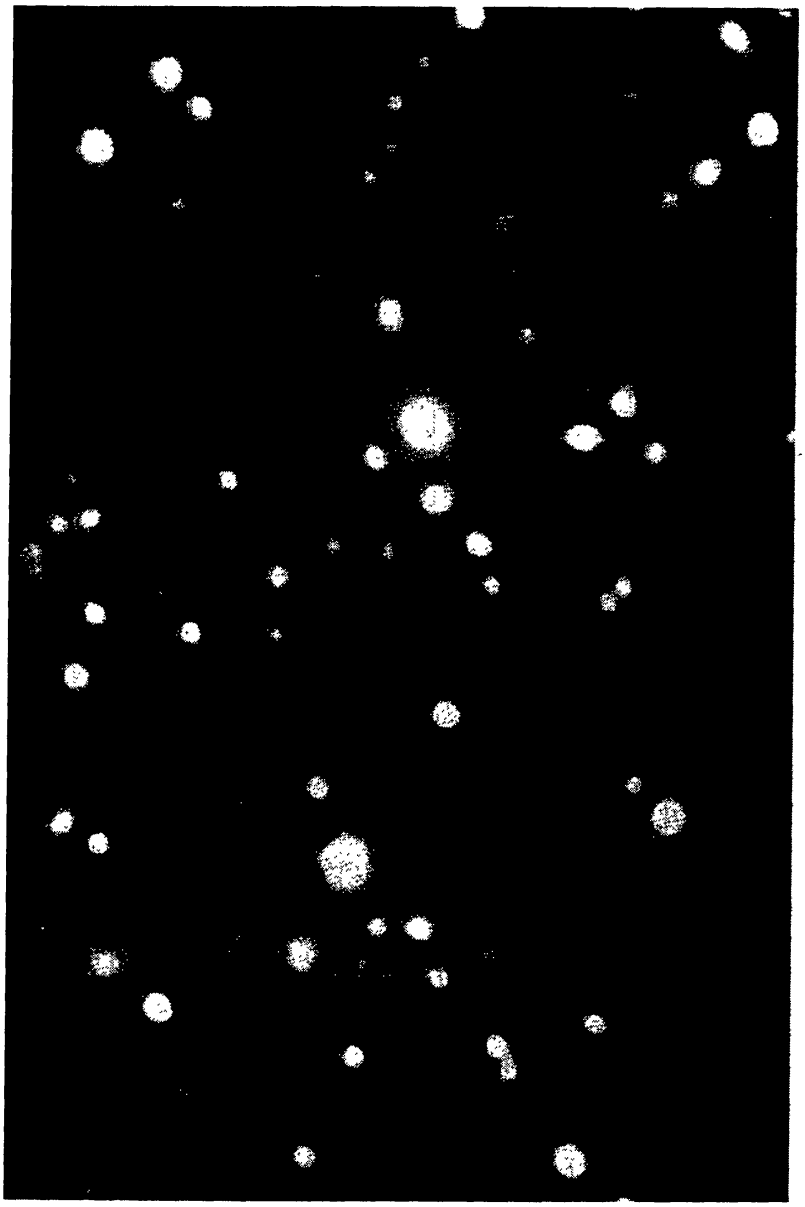

FIG. 2. Deep optical image of the rich cluster Abell 370 showing a prominent arc believed to be a gravitationally distorted image of a background galaxy. Six small 'arclets' seen in the same field are probably also distorted background galaxy images (cf. Fort *et al.* 1988). (Image courtesy of R.Lynds.)

demonstrated how much more one can learn when the source is extended, rather than quasi-stellar.

Over the decade since the discovery of the original double quasar, about eight more *probable* cases of multiple-imaged quasars, eight strong cases of arcs and one other radio ring have been discovered. In addition, there are about as many *possible* examples of multiple-imaging that have been proposed. (It is, in practice, quite hard to *prove* that lensing is occurring.)

1.2 *Uses of gravitational lenses*

Since their discovery, gravitational lenses have been heralded as important astronomical tools. Specifically, they can be probes of the dark matter found in the outer parts of galaxies, rich clusters of galaxies and perhaps also the Universe at large, It is a happy thought that we can use photons to probe the gravitational potential of a galaxy or cluster in much the same way that we use beams of relativistic electrons to explore an atomic nucleus. Following Refsdal (1964), lenses have also been welcomed as instruments for performing basic cosmography, specifically for measuring the Hubble constant and the deceleration parameter of the universe by monitoring the source variability in two or more of the images and by observing sources at two or more redshifts with the same lens. A third astronomical use of gravitational lenses is as giant telescopes. (An 8-m reflector seems pretty unambitious in comparison with a 100 kpc cluster of galaxies.) Suitably located sources can be magnified by large factors, perhaps exceeding several hundred, and this allows us to see intrinsically fainter sources as well as examine their internal structure and spectra. With the discovery of arcs and rings, this capability, which was anticipated many years ago by Zwicky, is beginning to be realized. Finally, by exploiting the stellar granularity in galactic lenses, it may be possible to probe regions within a quasar on scales of microarcseconds, finer than the angular resolution likely to be achieved directly within the foreseeable future.

Unfortunately, I have to admit that gravitational lenses have so far told us nothing reliable about the extragalactic universe that we did not already know. What they have done is tell us quite a lot about geometrical optics that, as astronomers, we ought to have known. Despite this, the main point I want to make in this lecture is that we should be optimistic that, over the next few years, gravitational lenses will start to fulfil their promise as astronomical tools. This is what happened with pulsars. It took a decade for astronomers to study how they worked before they started to be really useful as clocks, for testing relativity, as sources for scintillation and magnetoionic experiments, as probes of the interstellar medium, globular cluster dynamics and as fossil records of advanced stellar evolution and so on. I shall return to these possible uses below.

2 MULTIPLE IMAGING OF POINT-LIKE SOURCES

2.1 *Ray optics*

The optical arrangement is quite simple, involving a source S, usually a distant quasar or galaxy, a lens L, either a galaxy or a cluster of galaxies and the observer O (i.e. us). However, it differs in two key respects from the optics of a refracting telescope (Fig. 3). Firstly, the relation between the deflection and distance from the optic axis is usually highly non-linear, and somewhat non-circular (strong spherical aberration and astigmatism) leading to the formation of caustics rather than a point focus. As a consequence, there need no longer be a unique ray connecting a point source to each point on an image plane. Multiple images are possible, just as waves on the surface of a

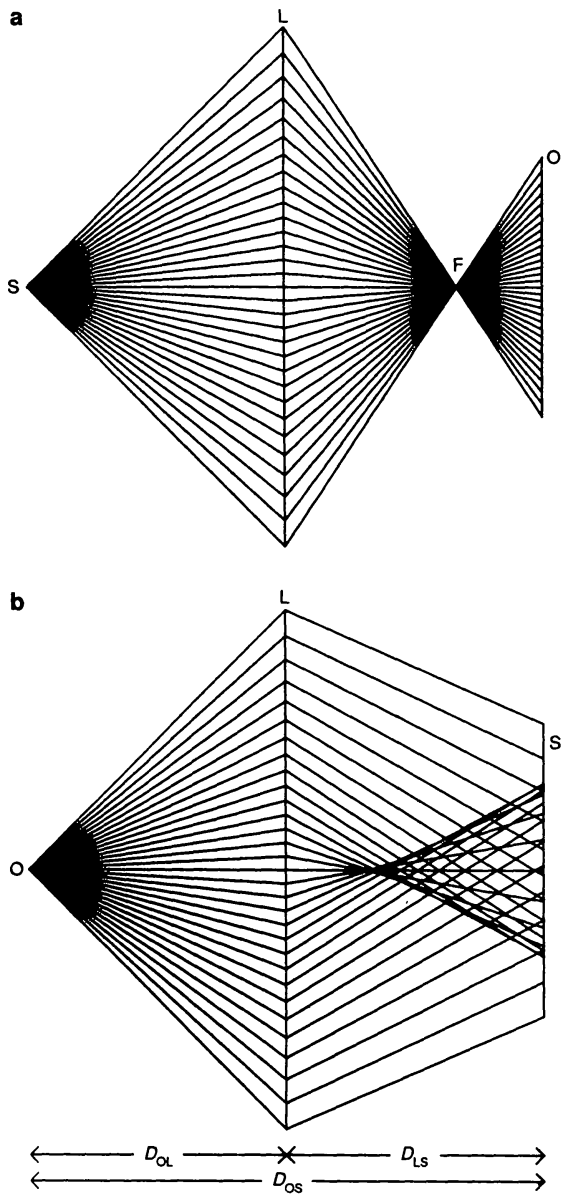

FIG. 3. Schematic representation of the difference between a linear lens and a non-linear gravitational lens. (a) Light from a source passes through a point focus F on its way to an observer at O. In general, just one ray connects the source to the observer. (b) Non-linear lens showing rays emanating from the observer and propagating backward in time through the lens to the source region. As the lens is non-linear, the focus unfolds to form a cusp caustic. When the source is located beyond the cusp, three images can be seen.

lake can form multiple images of the setting sun. Secondly, as our position is effectively fixed in space, it is more convenient to consider a point observer mapping onto source space rather than a point source mapping onto the image plane. We therefore trace rays backward in time in the scholastically approved manner.

2.2 *Fermat's Principle*

A convenient and elegant way to understand image formation, introduced by Nityananda, is to use Fermat's Principle (cf. Schneider 1985; Blandford & Narayan 1986). Let us consider a single lens plane and null geodesics connecting points on this plane (labelled by angular coordinates $\mathbf{r} \ll 1$ on the sky as seen by the observer) to both the source and the observer. Now let us use Eddington's refractive index to compute the travel time along the two geodesics relative to the travel time along a single geodesic in the absence of the lens.

$$t = (1+z_L)\left(\frac{D_{OS}D_{OL}}{2cD_{LS}}(\mathbf{r}-\boldsymbol{\rho})^2 - 2\int\frac{\varphi}{c^3}\mathrm{d}s\right), \tag{2}$$

where $\boldsymbol{\rho}$ labels the angular position of the source in its plane (in the absence of the lens). The first term just takes account of the extra distance light has to travel, the second is associated with the delay when passing through the gravitational potential well. The distances D_{ij} are angular diameter distances that connect the observer (O), lens (L) and source (S) and the redshift factor converts to observer time. In a Friedmann cosmology,

$$D_{ij} = \frac{2c}{\Omega_0^2 H_0}\frac{(G_iG_j+\Omega_0-1)(G_j-G_i)}{(1+z_i)(1+z_j)^2},$$

where $G_i = (1+\Omega_0 z_i)^{\frac{1}{2}}$, z_i is the redshift and H_0 is the Hubble constant. (Note that this distance measure is not symmetric in i,j because the universe is expanding.) The integral over the potential is recognized as the two-dimensional or surface potential. It is convenient to introduce a scaled time so that

$$\tau = \frac{cD_{LS}\,t}{(1+z_L)D_{OL}D_{OS}} = \tfrac{1}{2}(\mathbf{r}-\boldsymbol{\rho})^2 - \psi(\mathbf{r}),$$

where $\psi = 2D_{LS}\int\varphi\,\mathrm{d}s/c^2D_{OL}D_{OS}$ satisfies a two-dimensional Poisson equation

$$\nabla^2\psi = \frac{2\Sigma}{\Sigma_{crit}}.$$

The differentiation is with respect to $\mathbf{r}$. Σ is the surface density in the lens and $\Sigma_{crit} = c^2D_{OS}/4\pi GD_{OL}D_{LS}$ is the critical surface density sufficient for the formation of multiple images. Numerically, $\Sigma_{crit} \sim cH_0/4\pi G \sim 1\ \mathrm{g\ cm^{-2}}$, a useful rule of thumb!

Now, by Fermat's Principle, images of the source will be located where the travel time τ is stationary, i.e. where

$$\mathbf{r} = \boldsymbol{\rho} - \nabla\psi. \tag{3}$$

The second term on the right-hand side of this vector equation can be recognized as D_{LS}/D_{OS} times the deflection by the lens, and the equation can be immediately interpreted geometrically. This equation can be inverted to describe the one-to-many mapping from the source plane onto the image plane.

If we consider plotting contours of τ, then, in the absence of a lens, there

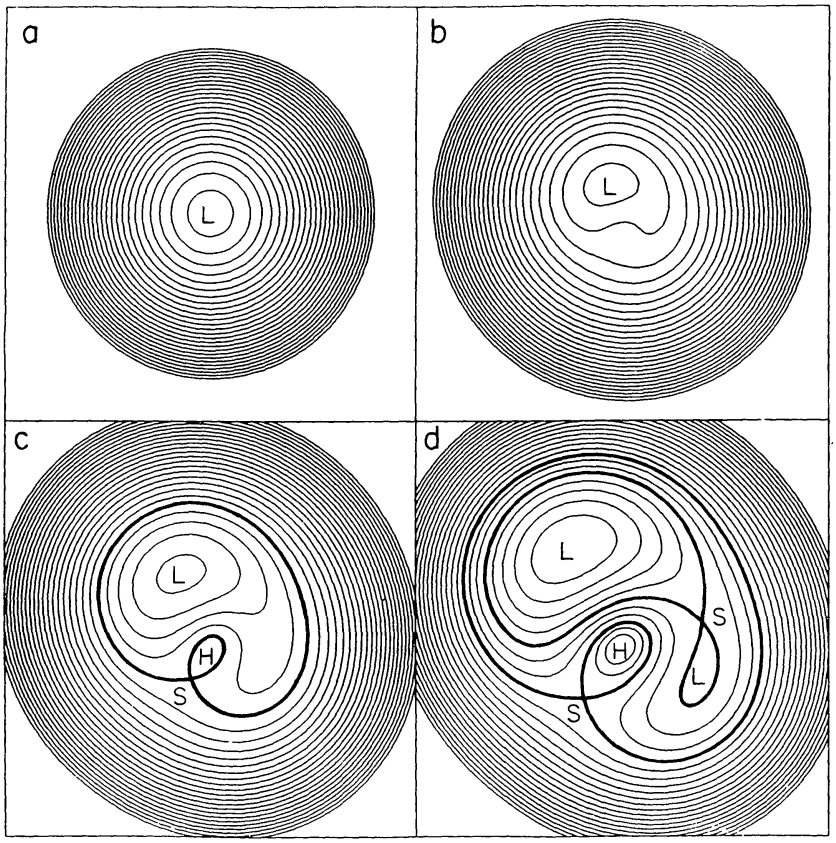

FIG. 4. Virtual arrival-time contours for single elliptical lens of increasing strength. Images are formed at the stationary points, lows, saddles and highs. The times at the stationary points measure the time delays that would be measured by an observer monitoring a variable source. It can be seen that only certain combinations of arrival time order and parity are allowed. (a) No lens. The single image is formed at the minimum of the paraboloidal time surface, corresponding to the rectilinear propagation of light. (b) A weak lens deflects this minimum. (c) An even stronger lens is able to create three images, a low, a saddle and a high, for which the separatrix has the shape of a limaçon. The image locations correspond to those observed in Q0957+561. (d) A stronger lens creates an additional low and saddle, with an extra separatrix in the shape of a lemniscate. The saddle and the low that are close to merging are very bright. This image arrangement is similar to that observed in PG1115+080. If the high and the other saddle were to merge then we would be left with an alternative three image topology to case (c).

will be a single minimum corresponding to the rectilinear propagation of light (Fig. 4). Adding a small mass displaces this minimum slightly away from the mass, corresponding to deflection of the ray. When a sufficiently large mass is introduced into the lens plane, extra stationary points will be formed in pairs, comprising a saddle and either a maximum or a minimum. We therefore see that a transparent, non-singular lens should form an odd number of images in total.

It is also possible to use this arrival time contour map to understand the magnification of images. As surface brightness is conserved through the lens, the flux magnification M is given by the ratio of the angular area of the image

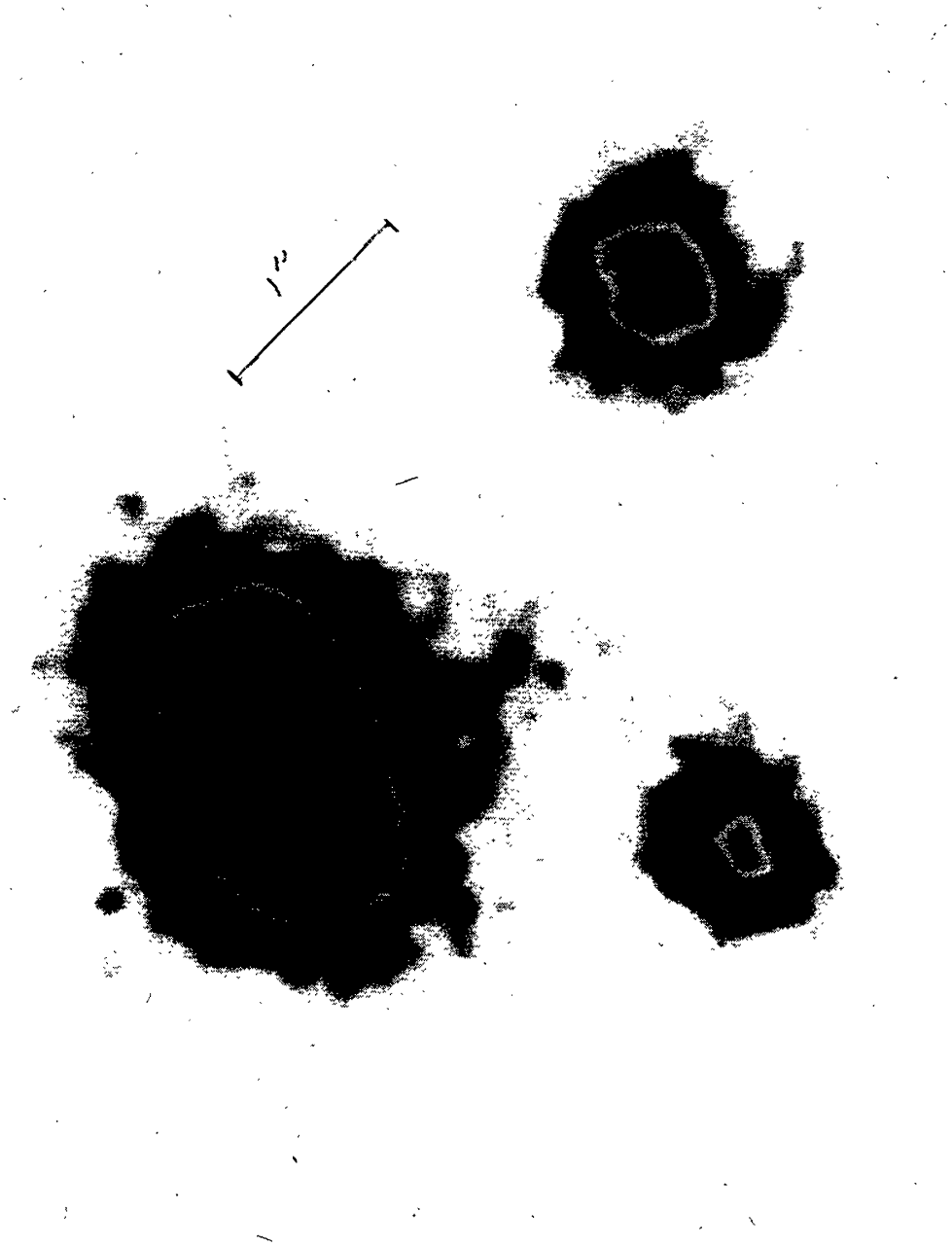

FIG. 5. Four images of the quasar PG1115+080 formed by an intervening galaxy. The bright elongated feature to the south west comprises two merging images. (CFHT prime focus image, courtesy J.Arnaud.)

to that of the source (assumed much smaller than any structure in the lens). In other words,

$$M^{-1} = \left|\left| \frac{\partial \boldsymbol{\rho}}{\partial \mathbf{r}} \right|\right| = \| \nabla_i \nabla_j \tau \|.$$

The magnification is therefore the reciprocal of the Gaussian curvature of the time delay surface, evaluated at the stationary points. Considering the arrival-time contours, we see that the surface is quite flat when two images

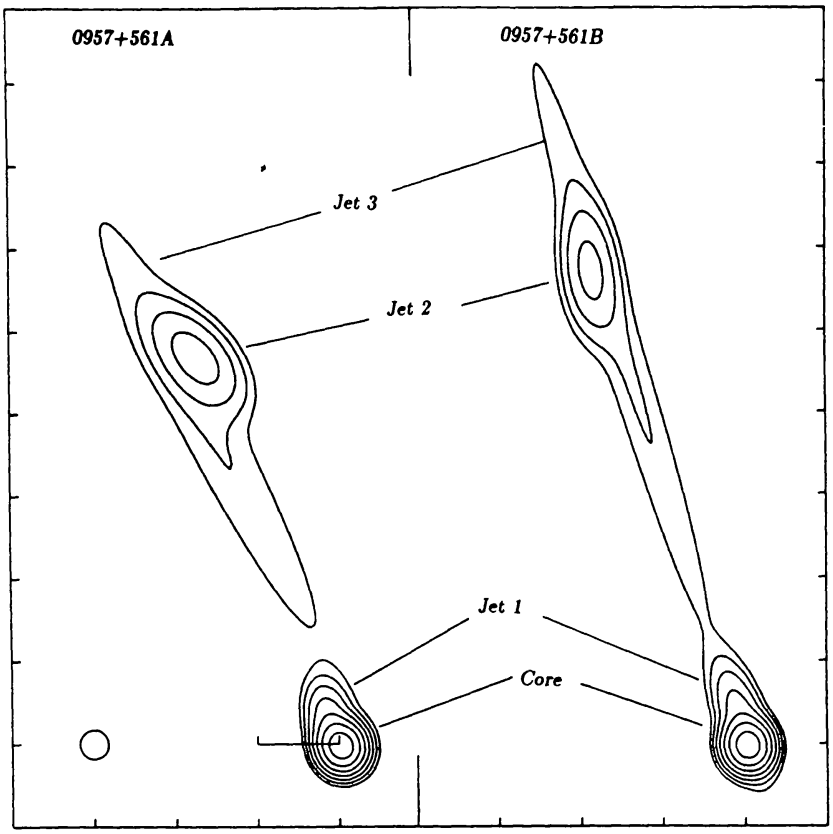

FIG. 6. Two VLBI images of the compact radio source associated with Q0957+561 (Gorenstein *et al.* 1988).

almost merge as in PG1115+080 (Fig. 5). The images are therefore very bright. Conversely, maxima located in the centres of lensing galaxies are likely to be highly curved, reflecting the shape of the gravitational potential well. The associated images will be highly de-amplified and probably not detected at all and this can account for the fact that, in practice, an even number of images is generally observed. Saddles correspond to negative parity images and maxima to images that have been inverted twice and consequently have positive parity. In Q0957+561, the two images A, B have radio counterparts that have been resolved using VLBI. These images have opposite parity as the gravitational lens model requires (Gorenstein *et al.* 1988) (Fig. 6). Now the heights of the stationary points are just the additional time delays so, if the source varies, then the order in which the images vary is associated with a particular ordering of the parities. The differences in the heights of these maxima are roughly θ^2 times a Hubble time or a few years. Given a good enough model of the lens, a measurement of the time delay can then be converted into an estimate of the Hubble constant. A time delay of 1·2 yr has been measured (Schild 1990; Vanderriest *et al.* 1989) for the double quasar, which is consistent with H_0 in the usual range. Unfortunately, this measurement is still somewhat controversial (Falco, Krolik & Shapiro 1990). However, even when the time delay is measured, it is hard to see how limited information about two images can be converted into a sufficiently accurate

lens model for this to give, say, a 10 per cent measurement of the Hubble constant. (One easy way to see the difficulty is to note that a uniform surface density of mass gives a parabolic contribution to the potential which is degenerate with a change in the Hubble constant.)

2.3 *Caustics*

Now, instead of just changing the strength of the lens, let us keep this fixed and allow the source to move in the source plane and watch the arrival-time contours deform. Occasionally, a saddle will approach either a minimum or a maximum and the arrival time surface will flatten. Both images will increase in flux until the magnification becomes formally infinite and then disappears. The locus of the merging images in the image plane is known as the *critical line*; the associated locus of the source plane is known as the *caustic*. Caustic lines divide the source plane into regions of image multiplicity differing by ± 2. There are two possible types of caustic when the source is confined to a plane: *folds* involving the merging of two images and *cusps*, where two folds meet. The number of neighbouring images changes from two to zero when the source crosses a fold, and from three to one at a cusp. Complex caustic networks, like those observed in a swimming pool, can be created when the lens comprises several masses (e.g. Wambganss, Paczyński & Katz 1989).

There are some simple asymptotic scaling laws associated with these two types of caustic. We can prove one of them as follows. Let us define H to be the reciprocal of the magnification M. H must vanish on the critical curve where the magnification becomes infinite. Now expand H in a Taylor series in distance x on the sky from the critical curve where $H = 0$. The leading term in the expansion is linear in x. (The sign denotes the parity of the image.) The cross-section for forming a pair of images both with magnification in excess of M, or equivalently having $|H| < 1/M$, is proportional to the associated area of the source plane. In other words,

$$\begin{aligned}\sigma(>M) &\propto \int_{|H|<M^{-1}} d^2\rho \\ &= \int H d^2 r \\ &\propto M^{-2}.\end{aligned}$$

Under quite general conditions, the probability of forming images magnified by more than M will diminish asymptotically as M^{-2}.

Now, it is observed that the number of quasars more luminous than some luminosity L increases $\propto L^{-2.5}$ for bright quasars. Therefore the majority of bright, multiply-imaged quasars should be highly magnified. This appears to be the case. This phenomenon goes by the name of *amplification bias* (Turner, Ostriker & Gott 1984). It explains qualitatively why surveys of the very brightest quasars have been relatively successful in finding multiple-imaged cases. However, when we look at fainter quasars, we find that the integral luminosity function only steepens $\propto L^{-1.5}$ and so amplification bias should not be important for fainter quasars (as also appears to be the case). This explains why reports of a large overdensity of $\sim 19^m$ quasars close to galaxies

(Webster *et al.* 1988) (strictly galaxies close to quasars) were treated with some scepticism (e.g. Narayan 1989).

When we examine the cusp catastrophe, we find that the cross-section for forming three images all magnified by more than M decreases as $M^{-2.5}$ and so cusp images ought not to show much amplification bias. Bright single images, as well as triple images can be formed when the source is located close to a cusp. When $M \gg 1$, we find that the cross-section for forming a magnified single image is sixteen times the cross-section for forming three images all magnified by more than M (Blandford, Kochanek & Soucail, unpublished). There are other scaling laws that become true asymptotically as the source approaches the cusp. Let us denote the fluxes of the three images by F_i, $i = 1, 2, 3$ and give them the signs of the image parities. We also denote the positions of the distances of the images from the symmetry axis by x_i. Then

$$\lim \sum_{i=1}^{3} x_i = 0,$$

$$\lim \sum_{i=1}^{3} F_i = 0,$$

$$\lim \sum_{i=1}^{3} x_i F_i = 0,$$

$$\lim \sum_{i=1}^{3} x_i F_i^3 = 0,$$

where the source point approaches the cusp in the limit. These scaling laws might find an application if a supernova exploded in a triply-imaged galaxy located close to a cusp (Kovner & Paczyński 1988).

The existence of these asymptotic relations means that we can infer quite a lot about the two-dimensional potential. In fact, by knowing just the positions and fluxes of three images, we can infer all three second derivatives of the two-dimensional potential ψ plus two of the third derivatives and one fourth derivative at the position of the cusp. This information should, in principle, be useful in constraining models of the mass distribution and, in particular, in helping to locate the dark mass.

Unfortunately, we do not yet have a good clean example of a simple cusp. Perhaps the closest we come is the oxymoronic 'straight arc' found in the cluster Abell 2390 by Pello (1990) (Fig. 7). However, here a galaxy is clearly present, causing the potential to be non-smooth on the scale of the separation of the images and we are not quite in the asymptotic regime where the above relations should hold.

So far, we have just considered caustic lines by examining the images formed by sources confined to a specific plane behind the lens. However, the distance to the source D_{OS} can also vary and so it is possible to generalize caustic lines to caustic surfaces (Fig. 8). These caustic surfaces divide space up into regions where 1, 3 and 5 images can be formed. The caustic surface comprises fold surfaces that meet at cusp lines or *ribs* (which can, themselves, meet at higher order catastrophe points). If we think of these caustic sources as being formed behind individual galaxies, then it is just those more distant

FIG. 7. 'Straight arc' discovered by Pello (1990) in the cluster Abell 2390. Three images of a galaxy with redshift $z = 0{\cdot}91$ appear to be formed by the galaxy and the cluster acting in concert. (CFHT image courtesy G.Soucail.)

quasars or galaxies that lie close to these surfaces that will be highly magnified and which create distinctive image arrangements.

There is a quite different, though no less illuminating way to visualize these caustic surfaces. Imagine a small bundle of rays, a *congruence* propagating backwards in time from the observer through the lens to the source region. Let the bundle have a circular cross-section to start with. If the rays just propagate through flat, empty space, then the area of this circle would just increase with the square of the distance. However, if the congruence passes through some matter, then gravitational focusing will cause its area to

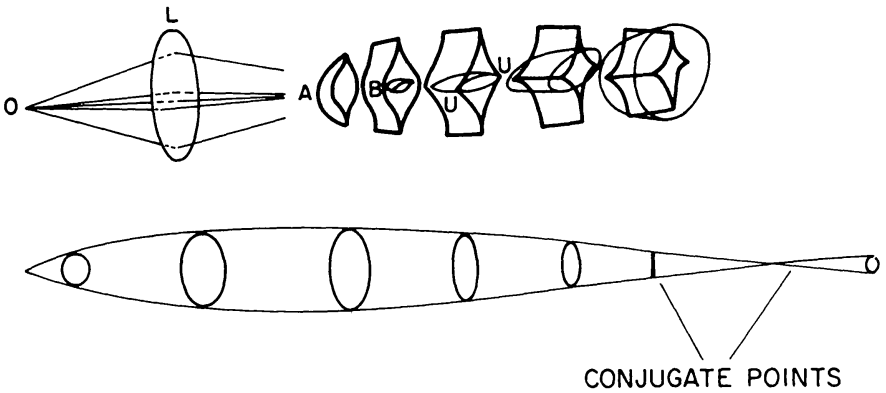

FIG. 8. Caustic surfaces formed by an elliptical lens. Two fold-surfaces form behind the lens terminated by cusp lines. They touch at a higher order catastrophe, *U*, known as a *hyperbolic umbilic*. Also shown is the evolution of a ray congruence propagating backward in time from the observer. The cross-section formed by the congruence degenerates to a line at two foci conjugate to us. The rays and the line are both tangent to the caustic surface at this point.

increase more slowly and can even cause it to decrease. In addition, matter lying outside the beam will deform the circular cross-section to an elliptical shape. The combination of both types of distortion, either distributed along the line of sight or localized in a lens plane, can eventually cause the cross-section to collapse to an ellipse of unit eccentricity, a line. This happens at a *conjugate point* to the observer. The amplification of a source located at a conjugate point will be infinite. The rays are tangent to the caustic surfaces at their conjugate points. The caustic surfaces are therefore the envelopes formed by these rays as they propagate backwards from the observer.

2.4 *Elliptical lenses*

Much work has been devoted to deriving detailed gravitational lens models for the various probable cases of multiple imaging. Most examples can be modelled successively though, for reasons to which I have already alluded, not uniquely. A simple elliptical lens model usually suffices. The image arrangements found typically have relatively large cross-sections (Fig. 9, Blandford & Kochanek 1987; Narayan & Grossman 1989).

2.5 *Microlensing*

Soon after the discovery of the first gravitational lens, it was realized that the granularity in the potential caused by the stars might create additional sub- or micro-images of a sufficiently compact source (e.g. Chang & Refsdal 1984; Schneider & Weiss 1988). Although these micro-images would be far too small to resolve, they might nevertheless cause a significant change to the integrated flux associated with the macro-image. The most dramatic changes occur when the source crosses a caustic formed by the interaction of the stellar and the background lens gravitational fields. As the caustic is crossed, the observed flux will rise to a value limited by the angular size of the source. Furthermore, as there will almost certainly be some relative transverse

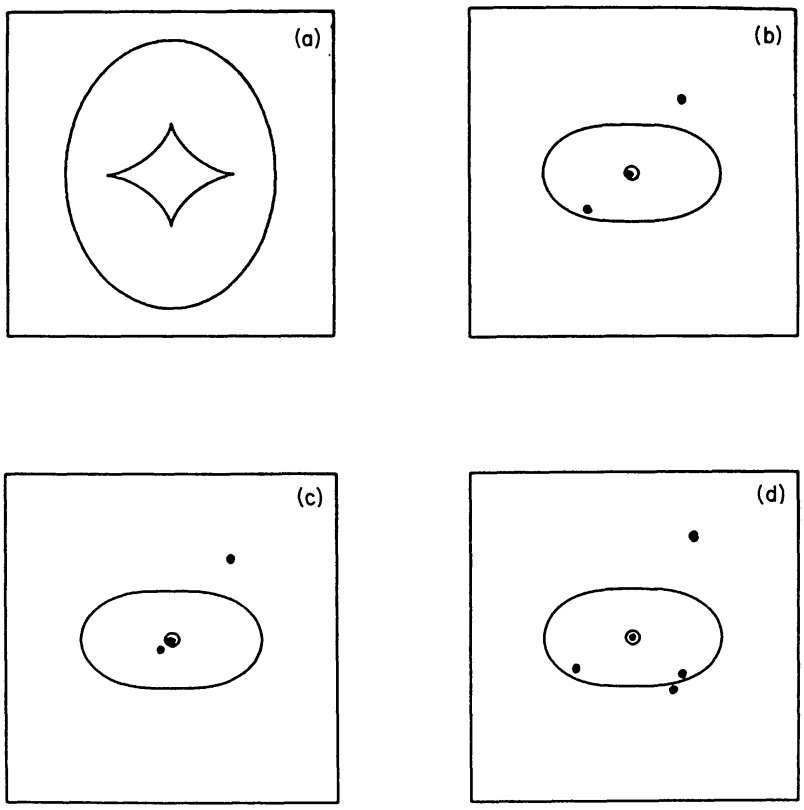

FIG. 9. Image arrangements produced by an elliptical gravitational lens. (a) Source plane. The caustics divide the source plane into regions where 1, 3 or 5 images are produced. In this case, the inner caustic has four cusp points joined by fold lines and a source within it will generate five images. As the ellipticity in the lens is reduced, this caustic shrinks to a point. The outer caustic separates the three image region from the single image region. (b) Critical curves and images in the image plane. When the source is located at b in the source plane, three images are formed. The brightest two are almost diametrically opposed. (c) When the source is located at c, the brightest two images are said to be 'allied' and straddle the smaller radial critical curve. (d) A source at d produces five images in total. In this example, the source is close to the caustic and the two brightest images are separated tangentially on either side of the outer critical curve.

motion between the stars and the line to the source, variability of the images will be induced. Now if a star of mass M is able to form micro-images, then the impact parameter of the ray is $b \sim (GMD/c^2)^{\frac{1}{2}}$ which is of order 10^{16} cm for solar type stars at cosmological distances. The probability that the flux be altered significantly by microlensing is called the optical depth $\tau \sim \Sigma_*/\Sigma_{\text{crit}}$, for $\tau \lesssim 1$. Here Σ_* is the surface density in stars. The time-scale for the flux to vary due to microlensing is $t_{\text{var}} \sim b/v_\perp$, where $v_\perp$ is the relative transverse velocity. Typically this is ~ 10 yr.

Although the phenomenon of microlensing has been invoked on many occasions, only recently has evidence been found of it actually occurring, and this in an environment where it is practically unavoidable. Corrigan *et al.* (1990) have reported a significant change in the brightest of the four images of the quasar 2237+035 that are formed by the nucleus of an intervening spiral galaxy (Fig. 10). We know that most of the mass in the nucleus is stellar

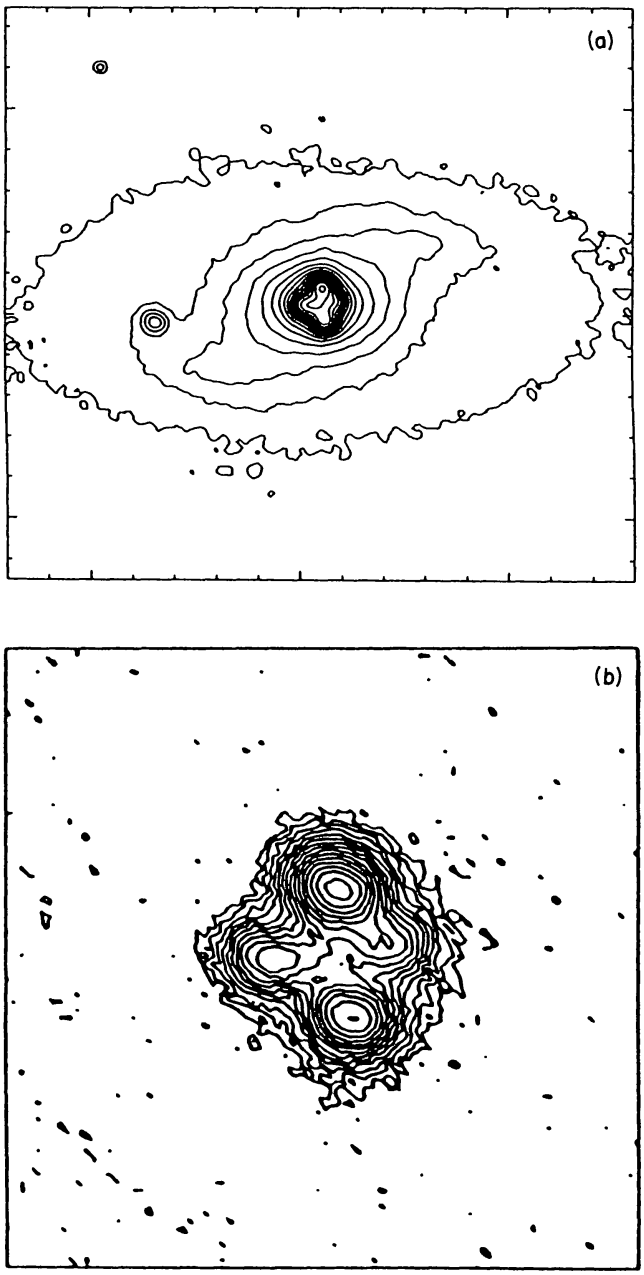

FIG. 10. (a) The quasar Q2237+0305 with a redshift $z = 1{\cdot}7$ seems to lie behind a $z = 0{\cdot}04$ spiral galaxy. (b) After the image processing of the central region, four images of the quasar have been identified. At least one of these images appears to vary significantly, probably caused by microlensing. (Images from Irwin *et al.* 1989.)

and can calculate that its surface density is about half the critical value. Provided that the source is sufficiently compact, independent large changes in luminosity should be seen in all four images with time-scales of about a year. These could be distinguished from variations intrinsic to the source for which the relative delays between the images should be typically about a week. Somewhat surprisingly, the variation observed occurs in a few months, which suggests that either the nucleus of the intervening galaxy contains very

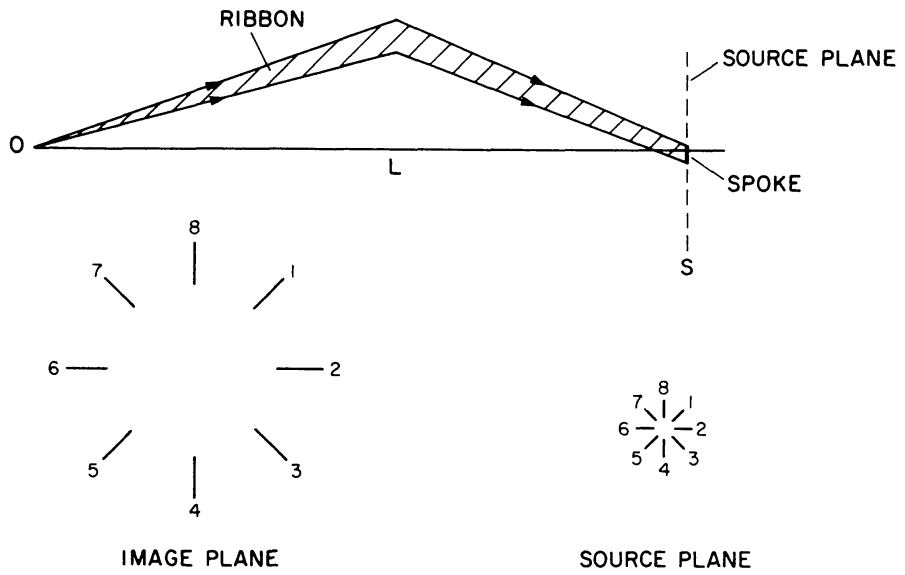

FIG. 11. Ribbons of rays propagating backwards from us past a circularly symmetric lens. The ribbons, labelled 1–8 intersect the source plane in radial spokes.

low mass stars or, once again, we have misunderstood some crucial point about the optics.

3 ARCS AND RINGS: IMAGING OF EXTENDED SOURCES

3.1 *Image formation by nearly circular lenses*

Although analysis of the location and fluxes of images of point sources can tell us quite a lot about the surface potential of the lens, we learn much more from the images of extended objects. This is because we can now sample the potential over an extended area rather than just at a few isolated points. In addition, the concern about microlensing affecting the magnification disappears. The spectacular discoveries of arcs and rings have transformed this into reality (Soucail *et al.* 1987; Lynds & Petrosian 1986; Hewitt *et al.* 1988). The acceptance of arcs as gravitational lens images was not immediate. (I, for one, argued that they were not lensed because I thought that a single long arc could not be produced by a cluster. This is incorrect, as I shall demonstrate.)

In order to understand how these images are formed, we should first consider image formation by a single circular, though non-linear, lens. Provided that the bending angle increases less rapidly than linearly with distance from the optic axis, there will be a single radius where a source located on the optic axis can form a ring image. This is known as the *Einstein radius* and the corresponding circle is the *Einstein ring* (Einstein 1936). The average surface density interior to this ring equals the critical density. Now let us trace a radial *ribbon* of rays backwards from the observer to the source plane. As the lens is circular, a short radial segment on the image plane cutting the Einstein ring, maps onto a short radial *spoke* on the source plane passing through the optic axis. We can map many such ribbons onto the

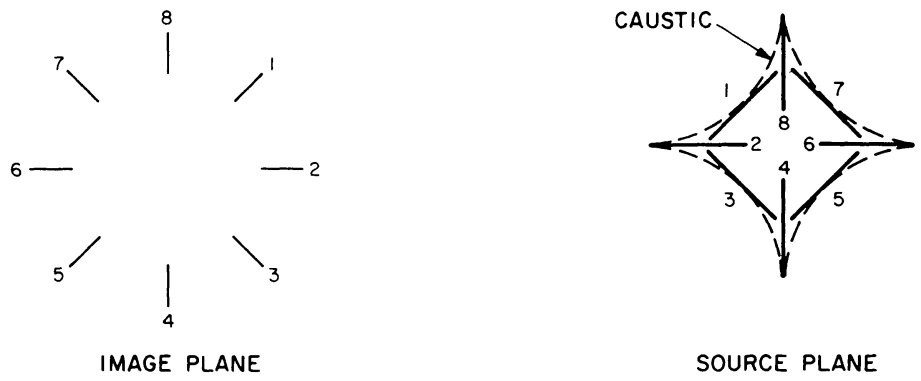

FIG. 12. As for Fig. 11, except that a small elliptical perturbation is introduced into the lens. The spokes in the source plane no longer pass through a common point and instead combine to form an astroid-shaped caustic envelope.

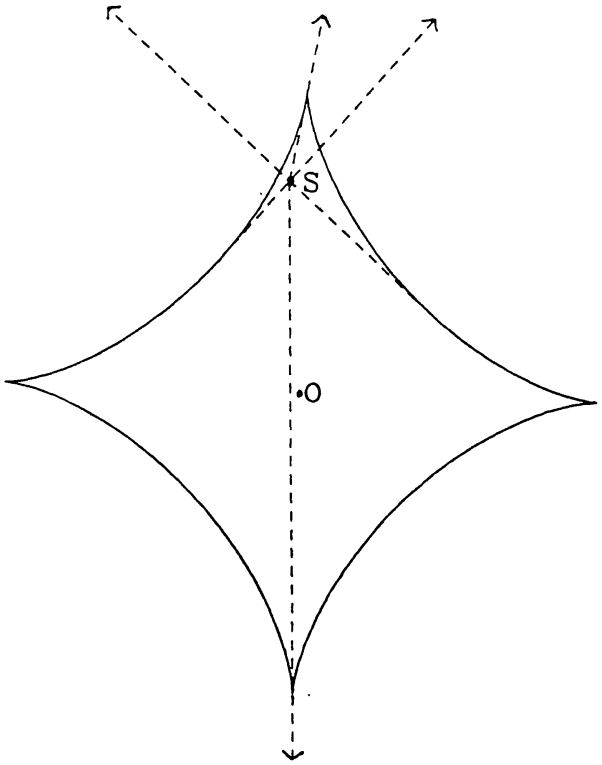

FIG. 13. Directions on the sky of images formed by a point source, S, located within an astroid caustic. The directions are tangent to the caustic and the images are located near to the Einstein ring.

source plane, each ribbon creating a spoke which passes through the optic axis when there is circular symmetry (see Fig. 11). Observe that an off-axis, extended source will create two arcs subtending equal angles at the optical centre of the lens.

The image arrangement from this type of lens is structurally unstable and if we introduce some small non-circularity into the lens, then the imaging changes significantly (Fig. 12). For an elliptical perturbation, the ribbons will be deflected slightly tangentially in a quadrupolar fashion as they cross the

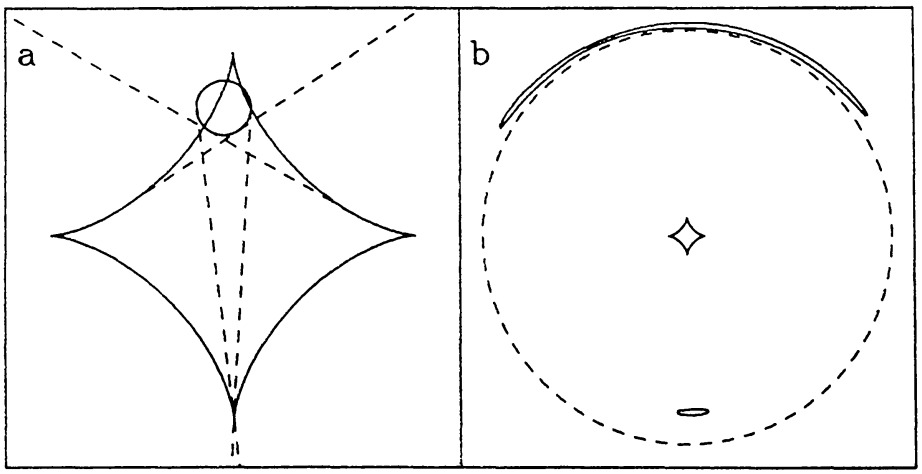

FIG. 14. Arc formation by an extended source. (a) In this example, a circular source is located close to a cusp and the directions of the images of the source points are bounded by drawing the common tangents to the caustic and the source. (b) Extent of the arc images near to the Einstein ring.

lens plane, giving similar transverse displacements to the spokes in the source plane. If we now superpose many spokes, their envelope forms a four-cusped astroid curve. (This is the caustic curve because any source point that lies on it maps onto two merging images near the Einstein ring.) This motivates an approximate geometrical construction for locating the images formed by an elliptical lens of a point source (Blandford & Kovner 1988; Fig. 13). Firstly, find the caustic curve on the sky and then draw all the tangents from the source position to the caustic and extend these tangents on the sky out to the original Einstein ring where the image points will be approximately located. When the source lies within an astroid caustic there will be four tangents and consequently four images; when it lies outside the astroid, there will be two tangents and therefore two images. If the source lies close to, and within, a cusp, then three nearby images will be created. The closer the source is to the caustic the closer are the images and the greater is their tangential magnification.

This construction can be used with extended sources as well (Fig. 14). It is simply necessary to construct the common tangents to the caustic and the source to determine the extent of the arc image. When the source overlaps the interior of a cusp, a large arc will be created. Those source points that lie within the cusp will be triply-imaged, those that lie outside will be singly-imaged. However, the tangents to the opposite cusp will extend only over a limited angle and only a small counter arc will be created. Sources that are not near to cusps create shorter arcs.

So, using this construction, we see how single long arcs can be produced by rich clusters of galaxies with large central surface densities.

3.2 *Arcs*

These features are similar to those seen in the observations of cluster arcs like the one in Abell 370. The sources are believed to be mostly high redshift,

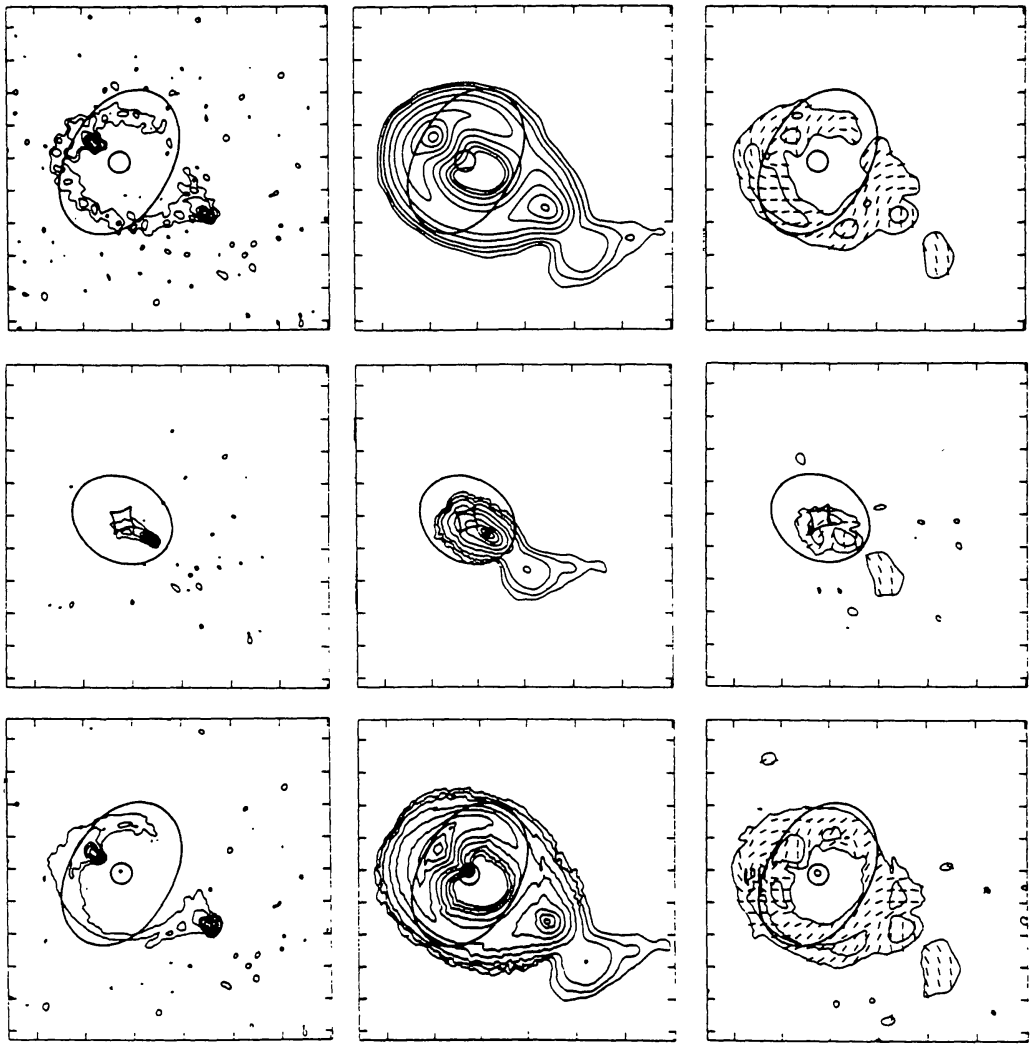

FIG. 15. Iterative inversion of the source structure in the radio ring MG1131+0456. The top map in the left column shows data at 15 GHz from Hewitt *et al.* (1988). The second map in this column shows the best-fitting source structure, and the bottom map shows the reconstructed image. The middle column shows data at 5 GHz processed using the same lens and the right-hand column shows 5 GHz polarization data. (Adapted from Kochanek *et al.* 1989.)

blue galaxies. As we have remarked, the images of extended sources constrain the lens models far more than the location and the amplification of individual images. It is therefore important to demonstrate that the observed arcs can indeed be reproduced by cluster lenses in which the mass has two components, one tracing the observed galaxies and the other representing the dark matter. This last is constrained so that the velocity dispersion of the galaxies has the observed value. It is found that arcs similar in shape and length to those observed can be reproduced in this manner, thereby strengthening our belief in the gravitational lens explanation (e.g. Grossman & Narayan 1988; Kovner 1988).

3.3 *Rings*

A similar explanation suffices for a qualitative understanding of the two known radio rings (MG1131+0456, Hewitt *et al.* 1988; MG1634+1346, Langston *et al.* 1989). Here, partial or complete ring images with angular diameters of a few arcseconds are formed of background radio sources by a radio-quiet, intervening galaxy lens.

A more sophisticated technique that my colleagues and I (Kochanek *et al.* 1989) have found to be very useful for the radio rings is to parameterize the lens model, using $\lesssim 10$ parameters, e.g. the ellipticity and orientation of the potential well. We then use the fact that the intensities of multiple images of individual source points should be identical. We can compute the dispersion in the intensity for these multiple image points for any suitable lens model. We then vary the lens parameters so as to minimize this dispersion. In this way, we can derive a best-fitting lens and source model (Fig. 15). We find that the resulting lens is capable of reproducing the radio structure observed at a second frequency as well as the polarization distribution (the polarization is parallel-propagated through the lens). This procedure also produces a quite plausible source structure. The method works fairly well for the radio rings because the lenses are relatively isolated. It should also be applicable to the cluster arcs, if and when they are observed with sufficient angular resolution.

4 FUTURE PROSPECTS

4.1 *Probes of dark matter*

The potential wells of galaxies and distant rich clusters appear to be formed by dark matter and it is naturally of interest to determine if this dark matter is distributed in a manner similar to the luminous material. Now the difficulty with galaxies is that they only have surface densities in excess of the critical value in their innermost parts, where dark matter is subdominant. Images formed by sources that lie behind the outer parts of galaxies will be only mildly distorted and will lack companion images. Attempts to measure the distortion of the images of more distant galaxies have not, as yet, been successful (e.g. Tyson *et al.* 1984). This imposes a fairly uninteresting limit on the galaxy masses.

There are now four large separation, possible double-imaged quasars. The best case for lensing is 1635+267, most recently studied by Turner *et al.* (1988) who found similarities in the emission line profiles of the two images and that the continua can be matched provided that a $z \sim 0{\cdot}6$, 20^m galaxy continuum is subtracted from the brighter spectrum. Unfortunately, the image separation is $\sim 4''$, too large to be created by an individual, normal galaxy. Furthermore, any galaxy located between the two images would have to be fainter than 23^m. If these images are from the same source, then the lens is surely not a normal galaxy. The proposal that this quasar pair is at least partly a 'dark matter lens' has now to be taken seriously, but this explanation cannot be accepted until some independent evidence for multiple imaging is uncovered. The alternative conclusion, that the two quasars are distinct and belong to the same group, is no less interesting as the upper limit

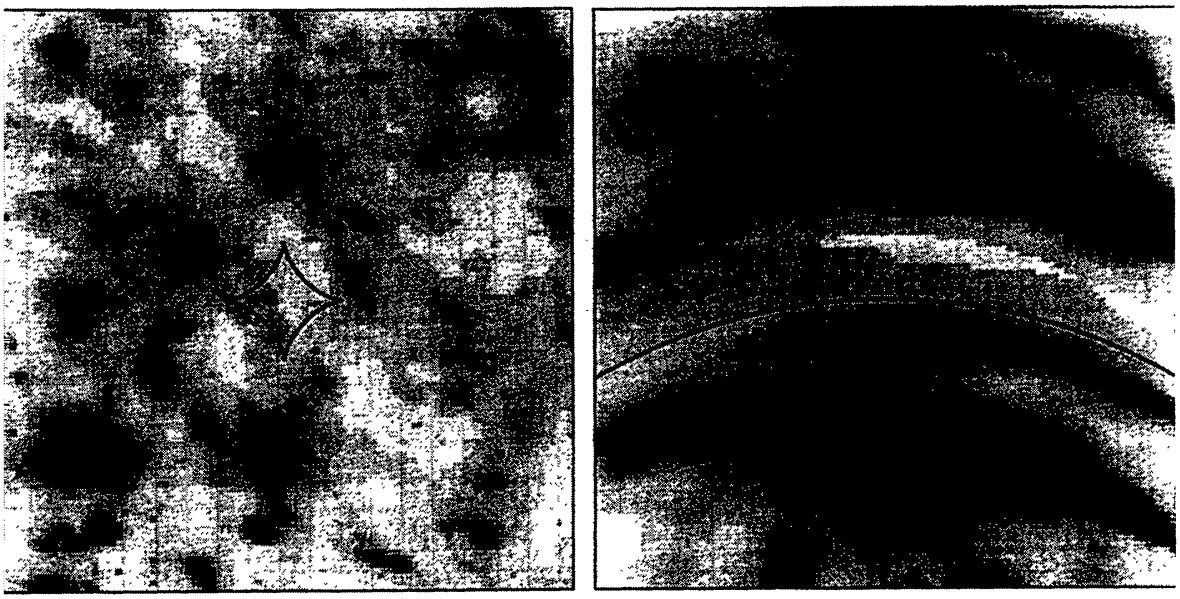

FIG. 16. (a) Simulated extended source structure produced by the superposition of 500 uncorrelated Gaussians in the source plane. The astroid caustic of an associated elliptical lens is shown as a bold curve. (b) Derived image structure, smoothed to simulate the finite angular resolution of the observation. Note the strong shear in the images close to the critical curve, also shown as a bold line.

on the velocity difference can be used to place an upper bound on the quasar masses ($\lesssim 10^{11}\,M_{\odot}$).

The situation with rich clusters of galaxies is quite promising. Recent studies of the original arc cluster, Abell 370, have demonstrated the existence of several faint secondary 'arclets', that are elongated tangentially with respect to the cluster centre, just as might be expected if the cluster is approximately circular-symmetric. This pattern is repeated in deep images of a few more clusters. Even more dramatically, Tyson, Valdes & Wenk (1990) have reported finding the pattern of small distortions in background galaxies, that they originally sought around galaxies in two rich clusters.

This observation both verifies that the blue galaxies are cosmologically distant and demonstrates how their images can sample the surface potential of clusters. In fact, Tyson *et al.* (1990) have shown that the centre of the dark matter distribution coincides with the centre of the light distribution and tentatively conclude that the radial distributions are also similar. Although these results are only preliminary, we can look forward to this technique being applied to many more clusters in the near future.

4.2 *Cosmography*

As we have discussed, it is going to be quite difficult to obtain an accurate measurement of the Hubble constant by cross-correlating the variations in two quasar images, mainly because there is too little information to constrain the lens model sufficiently. The difficulties are ameliorated with the radio rings. In particular, the potential is probably quite simple because it appears

that individual isolated galaxies are involved. In addition, the lens model can be determined highly redundantly, especially if the critical curve can be traced on the sky using high resolution VLBI images. This may be quite easy because when an amorphous but isotropic radio source is observed behind a nearly circular lens galaxy, there is a very striking anisotropy in the image close to the critical curve (see Fig. 16). Unfortunately, neither of the existing radio rings is ideal for this purpose. MG1131+0456 does contain a doubly-imaged compact radio core which may turn out to be variable. However, it has not proved possible to measure the redshift of the source and the lens. The second source, MG1634+1346, is mainly an image of a background extended radio source. Although the redshifts are known, the central component is only singly imaged. Ideally, what is needed is a ring image of a compact radio source, including a variable core, created by an intervening, isolated galaxy, where both redshifts are measured. If, in addition, the core is bright enough for VLBI observation and has moving components, then extra-rapid superluminal motion may be observed.

It will be much harder to measure Ω_0 in this way because there is only a weak variation of the time delay with Ω_0 for given source and lens redshifts. In principle, the distribution of observed lensing sources in redshift is sensitive to Ω_0. However, this will be subject to the traditional evolutionary corrections familiar from alternative methods.

4.3 *Giant telescopes*

The reconstruction of the source from the image of MG1131+0456 has already demonstrated a rather prosaic use of a natural telescope. The angular resolution obtained is superior to that which could be obtained directly using the VLA (though not by using VLBI). Rather more dramatic possibilities open up if the VLBA is used to make a high dynamic range map of the radio ring image. This is because the maximum effective magnification will be much larger than the typical magnification. For a fold caustic, the maximum gravitational magnification achievable, close to the critical curve, is roughly the ratio of the radius of the Einstein ring to the angular resolution of the radio telescope, perhaps several thousand. For a cosmologically distant source, this is equivalent to a linear resolution of perhaps 30 AU. In effect, we may be able to look at a small patch of a distant radio source with a similar linear resolution to that achievable when viewing the centre of our Galaxy. (Despite these impressively small dimensions, geometrical optics are still valid and the 'telescope' is not diffraction-limited.)

The prospects for finding more radio rings are quite good (Blandford 1989; Kochanek & Lawrence 1990). There are roughly 2×10^8 bright galaxies out to a redshift $z \sim 0{\cdot}5$ and their Einstein rings cover a fraction $f \sim 10^{-3}$ of the sky. If their typical ellipticities are $\varepsilon \sim 0{\cdot}1$, the fraction of the sky covered by their tangential caustics will be $\sim f\varepsilon \sim 10^{-4}$. Therefore, several radio rings ought to be found in existing radio catalogues.

So far, none of the cluster arcs has turned out to be a detectable radio source, which is not very surprising. However, it is possible that some of the brighter arcs may be imaged by HST; linear resolution as small as 1 pc is achievable, in principle, close to the critical curve.

The alternative, indirect way to use a gravitational lens telescope is to use microlensing to probe the source structure. With the tentative discovery of this effect in 2237+0305, it may be possible to test our notions of quasar source structure. The most common contemporary model of the quasar associates the continuum with an accretion disk, the blue and ultraviolet emission originating from the innermost parts, perhaps from radii $\sim 10^{15}$ cm, the red and yellow emission coming from intermediate radii and the infrared being re-radiated by dust at distances $\sim$ several pc from the central continuum source. Emission lines are believed to be formed at several pc from the ultraviolet continuum source. Now, somewhat surprisingly, the relative magnification of the optical image appears to vary in a few months. If we attribute this mainly to ~ 300 km sec^{-1} stellar motions in the core of the lensing galaxy then we deduce that the source size is $\lesssim 2 \times 10^{15}$ cm. This is still somewhat tentative, but it is clearly possible to test the above model of quasar structure by monitoring quasar variability in different wavebands. Perhaps the most dramatic effects will be seen at X-ray energies after a suitably located, X-ray loud quasar is discovered.

4.4 *A 'blue skies' proposal*

In conclusion, I would like to discuss a speculative application of gravitational imaging to cosmology. Let me start by flying in the face of established theory and entertaining the hypothesis that the Universe is as observed: the 'WYSIWYG' cosmology (WYSIWYG is an inelegant acronym from computer science for 'What you see is what you get'!) Recently, Geller & Huchra (1989) have presented results from the largest redshift survey to date, and have argued that bright galaxies are concentrated on relatively thin surfaces which appear to surround large voids. They find the void size to be typically $60\,h^{-1}$ Mpc and the thickness of the surrounding sheets to be $\sim 5\,h^{-1}$ Mpc where h is the Hubble constant in units of 100 km sec^{-1} Mpc^{-1}. The galaxy density in the sheets appears to be about five times the mean density. In addition, Geller and Huchra argue from measured cluster and group velocity dispersions that the cosmological density parameter is only $\sim 0{\cdot}2$, significantly less than the value of unity favoured by believers in inflation. Further evidence for large density inhomogeneities has been derived using empirical distance indicators (e.g. Lynden-Bell *et al.* 1988) to deduce substantial departures from the Hubble flow.

If these giant inhomogeneities exist, they can have a measurable influence on the images of background objects seen through them (cf. Valdes, Tyson & Jarvis 1983; Dyer & Oattes 1988). In particular, images will be sheared in a correlated fashion over large areas of sky. If we trace null geodesic congruences backwards in time, we find that circular cross-sections will be deformed into ellipses by the tidal gravitational forces exerted by the large clumps and sheets of matter that we are hypothesizing. (This is the closest I come to the scientific interests of Sir George Darwin.) The ellipticity induced in the images of circular sources will be

$$\varepsilon \sim \Omega_c \left(\frac{LH_0}{c}\right)^{\frac{1}{2}}, \tag{4}$$

where L is the correlation length of the large-scale structure and Ω_c is the fraction of the critical density that is inhomogeneous on this scale. Now for $\Omega_c \sim 0{\cdot}2$, $L \sim 60\,h^{-1}$ Mpc, this gives $\varepsilon \sim 0{\cdot}03$. (For a cold dark matter cosmology, $\varepsilon \sim 10^{-3}$.)

As we have described, there appears to be a dense population of faint blue galaxies with redshifts in the range $1 \lesssim z \lesssim 3$ (Tyson 1988). They are estimated as having a surface density of $\sim 2 \times 10^5$ per square degree down to a blue magnitude $m_B \sim 27$ and a surface brightness of 29 magnitudes in each square arc second, about 10^{-3} the surface brightness of the night sky in this waveband. The galaxies appear to cover about 15 per cent of the sky at this surface brightness and are about 7″ apart on the average with a median size of about 3″.

A large solid angle of sky can now be surveyed with CCDs with fields of view as large as 50′ (Tyson, private communication) and image processing software exists to measure and collate the ellipticities of these supposed galaxies in a manner akin to what has already been successfully applied behind rich clusters (Tyson, Valdes & Wenk 1990). Suppose that the ellipticities and orientations of individual galaxies can be measured with an accuracy $\sim 0{\cdot}3$ over a solid angle $\Delta\Omega \sim LH_0/c \sim 1°$. Then it should be possible to measure the mean induced ellipticity to an accuracy $\sim 10^{-3}$, sufficient to test a 'WYSIWYG' cosmology.

5 CONCLUSION

I hope that in this talk I have been able to convey some of the accomplishments and current interest of research into gravitational lenses over the past decade. I also hope that I have been able to persuade you that it is now time for these objects to start fulfilling their promise as astronomical tools. In particular, I want to advertise the benefits of photons, not just as conveyers of information, but as powerful probes of the disposition of mass in the universe. In this respect, they have several advantages over galaxies. They are plentiful, we know their three-dimensional velocities very accurately, they do not interact with each other and their observed properties are not dependent upon such ill-defined processes as dynamical friction, gas dynamics and star formation rates. A considerable amount of telescope time will continue to be requested to use gravitational lenses to full advantage but the scientific benefits that should follow are considerable.

ACKNOWLEDGMENTS

I thank the Royal Astronomical Society for the invitation to deliver this lecture, Professors G.Efstathiou and M.Rees for hospitality during its preparation. I thank them and E.Falco, B.Fort, P.Hewett, S.Refsdal, R.Smith R.Tayler and J.Tyson for helpful service and editorial assistance. I also acknowledge the financial support of the National Science Foundation under grant AST 86-15325.

REFERENCES

Barnothy, J., 1965. *Astr. J.*, **70**, 666.
Blandford, R.D., 1989. *Gravitational Lenses*, eds Moran, J.M., Hewitt, J.N. & Lo, K.Y., Springer-Verlag, Berlin.
Blandford, R.D. & Kochanek, C.S., 1987. *Astrophys. J.*, **321**, 658.
Blandford, R.D. & Kovner, I., 1988. *Phys. Rev. A*, **38**, 4028.
Blandford, R.D. & Narayan, R., 1986. *Astrophys. J.*, **310**, 568.
Bourrassa, R.R. & Kantowski, R., 1975. *Astrophys. J.*, **195**, 13.
Chang, K. & Refsdal, S., 1984. *Astr. Astrophys.*, **132**, 168.
Chwolson, O., 1924. *Astr. Nachrichten*, **221**, 329.
Corrigan, R.T., Irwin, M.J., Hewitt, P.C. & Webster, R.L., 1990. *Toulouse Workshop on Gravitational Lenses*, eds Fort, B., Mellier, Y. & Soucail, G. Observatoire du Pic-du-Midi et de Toulouse (in press).
Dyer, C.C. & Oattes, LM., 1988. *Astrophys. J.*, **326**, 50.
Dyson, F.W. 1919. *The Observatory*, **42**, 389.
Eddington, A.S., 1919. *The Observatory*, **42**, 119.
Einstein, A., 1936. *Science*, **84**, 506.
Falco, E., Krolik, J.H. & Shapiro, I.I., 1990. *Toulouse Workshop on Gravitational Lenses*, eds Fort, B., Mellier, Y. & Soucail, G. Observatoire du Pic-du-Midi et de Toulouse (in press).
Fort, B., Prieur, J.L., Mathes, Y., Mellier, Y. & Soucail, G., 1988. *Astr. Astrophys.*, **200**, L17.
Geller, M.J. & Huchra, J.P., 1989. *Science*, **246**, 897.
Gorenstein, M.V., Cohen, N.L., Shapiro, I.I., Rogers, A.E.E., Bonometti, R.J., Falco, E.E., Bartel, N. & Marcaide, J.M., 1988. *Astrophys. J.*, **334**, 42.
Grossman, S. & Narayan, R., 1988. *Astrophys. J. (Lett.)*, **324**, L37.
Hewitt, J.N., Turner, E.L., Schneider, D.P., Burke, B.F., Langston, G.I. & Lawrence, C.R., 1988. *Nature*, **333**, 537.
Irwin, M.J., Webster, R.L., Hewett, P.C., Corrigan, R.T. & Jedrzejewski, R.I., 1989. *Astr. J.*, **89**, 1989.
Klimov, Yu.G., 1963. *Soviet. Phys.*, **8**, 119.
Kochanek, C.S., Blandford, R.D., Lawrence, C.R. & Narayan, R., 1989. *Mon. Not. R. astr. Soc.*, **238**, 43.
Kochanek, C.S. & Lawrence, C.R., 1990. *Mon. Not. R. astr. Soc.* (in press).
Kovner, I., 1988. *The Post-Recombination Universe*, eds Kaiser, N. & Lasenby, A.N., Kluwer Academic Press, Boston, U.S.A.
Kovner, I. & Paczyński, B., 1988. *Astrophys. J. (Lett.)*, **335**, L9.
Langston, G.I., Schneider, D.P., Conner, S., Lehar, J., Carilli, C.L., Burke, B.F., Gunn, J.E., Hewitt, J.N., Turner, E.L. & Schmidt, M., 1989. *Astr. J.*, **97**, 1283.
Liebes, S., 1964. *Phys. Rev.*, **133**, B835.
Lodge, O., 1919a. *The Observatory*, **42**, 365.
Lodge, O., 1919b. *Nature*, **104**, 354.
Lynden-Bell, D., Faber, S.M., Burstein, D., Davies, R.L., Dressler, A., Terlevich, R.J. & Wegner, G., 1988. *Astrophys. J.*, **326**, 19.
Lynds, R. & Petrosian, V., 1986. *Bull. Amer. Astr. Soc.*, **18**, 1014.
Narayan, R., 1989. *Astrophys. J. (Lett.)*, **339**, L53.
Narayan, R. & Grossman, S., 1989. *Gravitational Lenses*, eds Moran, J.M., Hewitt, J.N. & Lo, K.-Y., Springer-Verlag, Berlin.
Paczyński, B., 1987. *Nature*, **325**, 572.
Pello, R., 1990. *Toulouse Workshop on Gravitational Lenses*, eds Fort, B., Mellier, Y. & Soucail, G. Observatoire du Pic-du-Midi et de Toulouse (in press).
Porcas, R.W., Booth, R.S., Browne, I.W.A., Walsh, D. & Wilkinson, P.N., 1981. *Nature*, **289**, 758.
Press, W.H. & Gunn, J.E., 1973. *Astrophys. J.*, **185**, 397.
Refsdal, S., 1964. *Mon. Not. R. astr. Soc.*, **128**, 295.
Schild, R., 1990. *Toulouse Workshop on Gravitational Lenses*, eds Fort, B., Mellier, Y. & Soucail, G. Observatoire du Pic-du-Midi et de Toulouse (in press).
Schneider, P., 1985. *Astr. Astrophys.*, **143**, 413.
Schneider, P. & Weiss, A., 1988. *Astrophys. J.*, **327**, 526.
Soucail, G., Fort, B., Mellier, Y. & Picat, J.-P., 1987. *Astr. Astrophys.*, **172**, 414.

Turner, E.L., Ostriker, J.P. & Gott, J.R., 1984. *Astrophys. J.*, **284**, 1.
Turner, E.L., Hillenbrand, L.A., Schneider, D.P., Hewitt, J.N. & Burke, B.F., 1988. *Astr. J.*, **96**, 1682.
Tyson, J.A., 1988. *Astr. J.*, **96**, 1.
Tyson, J.A., Valdes, F., Jarvis, J.F. & Mills, A.P., 1984. *Astrophys. J.* (*Lett.*), **281**, L59.
Tyson, J.A., Valdes, F. & Wenk, R.A., 1990. *Astrophys. J.* (*Lett.*), **349**, L1.
Valdes, F., Tyson, J.A. & Jarvis, J.F., 1983. *Astrophys. J.*, **271**, 431.
Vanderriest, C., Schneider, J., Herpe, G., Chevreton, M., Moles, M. & Wlerick, G., 1989. *Astr. Astrophys.*, **215**, 1.
Walsh, D., 1989. *Gravitational Lenses*, eds Moran, J.M., Hewitt, J.N. & Lo., K.-Y., Springer-Verlag, Berlin.
Walsh, D., Carswell, R.F. & Weymann, R.J., 1979. *Nature*, **279**, 381.
Wambganss, J., Paczyński, B. & Katz, J., 1989. *Gravitational Lenses*, eds Moran, J.M., Hewitt, J.N. & Lo, K.-Y., Springer-Verlag, Berlin.
Wayman, P.A. & Murray, C.A., 1989. *The Observatory*, **109**, 189.
Webster, R.L., Hewett, P.C., Harding, M.E. & Wegner, G.A., 1988. *Nature*, **336**, 358.
Young, P.J., Gunn, J.E., Kristian, J., Oke, J.B. & Westphal, J.A., 1980. *Astrophys. J.*, **241**, 507.
Young, P.J., Gunn, J.E., Kristian, J., Oke, J.B. & Westphal, J.A., 1981. *Astrophys. J.*, **244**, 736.
Zwicky, F., 1937. *Phys. Rev. Lett.*, **51**, 290.